Biochimica et Biophysica Acta 1798 (2010) 1724–1734

Contents lists available at ScienceDirect

Biochimica et Biophysica Acta

journal homepage: www.elsevier.com/locate/bbamem

Numerical studies of the membrane fluorescent dyes dynamics in ground and excited states

Justyna Barucha-Kraszewska [a], Sebastian Kraszewski [b], Piotr Jurkiewicz [a], Christophe Ramseyer [b,*], Martin Hof [a]

[a] Ústav fyzikální chemie J. Heyrovského AV ČR, v. v. i., Dolejškova 2155/3, 182 23 Praha 8, Czech Republic
[b] Institut UTINAM, Université de Franche-Comté, 16 Route de Gray, 25000 Besançon, France

ARTICLE INFO

Article history:
Received 7 January 2010
Received in revised form 17 May 2010
Accepted 19 May 2010
Available online 25 May 2010

Keywords:
Molecular dynamics
Fluorescent probe
Membrane
Excited state
Solvent relaxation
Prodan
Laurdan

ABSTRACT

Fluorescence methods are widely used in studies of biological and model membranes. The dynamics of membrane fluorescent markers in their ground and excited electronic states and correlations with their molecular surrounding within the fully hydrated phospholipid bilayer are still not well understood. In the present work, Quantum Mechanical (QM) calculations and Molecular Dynamics (MD) simulations are used to characterize location and interactions of two membrane polarity probes (Prodan; *6-propionyl-2-dimethylaminonaphthalene* and its derivative Laurdan; *2-dimethylamino-6-lauroylnaphthalene*) with the dioleoylphosphatidylcholine (DOPC) lipid bilayer model. MD simulations with fluorophores in ground and excited states are found to be a useful tool to analyze the fluorescent dye dynamics and their immediate vicinity. The results of QM calculations and MD simulations are in excellent agreement with available experimental data. The calculation shows that the two amphiphilic dyes initially placed in bulk water diffuse within 10 ns towards their final location in the lipid bilayer. Analysis of solvent relaxation process in the aqueous phase occurs on the picoseconds timescale whereas it takes nanoseconds at the lipid/water interface. Four different relaxation time constants, corresponding to different relaxation processes, where observed when the dyes were embedded into the membrane.

1. Introduction

Lipid bilayer is a main element of biological membranes that ensures its integrity and controls functions of membrane proteins [1–4]. In addition, the lipid bilayer is a suitable supramolecular model possessing attributes of complex systems in which a number of processes take place simultaneously at the same place but at different time scales [5]. Fluorescence techniques are convenient experimental tools to study lipid bilayers due to the existence of variety of fluorescent probes and methods able to gather data in broad range of time scales [6]. Fluorescence studies of the lipid bilayer relay on dedicated fluorescent probes interacting with the aggregate. The necessity to use a probe raises serious issues of probe effect on the studied structure. In addition, the probe reports on its immediate vicinity, which requires additional information in order to correctly interpret the experimental data. There are two major issues; the precise knowledge of the probe location and the correlation of the signal coming out of the probe with the specific lipid bilayer property. The first issue was addressed with dedicated experimental techniques [7,8] whereas the second is not yet satisfactory resolved. It is worth noting that there are number of fluorescence techniques to study various properties of the lipid bilayer, including dynamical and chemical quenching [6,9–12], energy transfer [12,13], dye adsorption [14,15], lifetime distribution [6,16], excimer formation [17,18] or anisotropy [6]. All of these techniques are usually averaged throughout the population of dyes and time and are reflecting the change of probe properties, which need to be later interpreted in term of lipid bilayer properties. However, there are also methods that probe directly selected membrane properties, e.g. fluorescent solvent relaxation (SR) [19–23], general polarization (GP) [24], and red edge excitation shift (REES) [25,26]. These ones report on the level of local hydration and mobility depending on the fluorescent probe location. They are somewhat complementary but SR technique seems to be more informative. Solvent relaxation is indeed mostly used for studying hydration and mobility of the phospholipid headgroups [22]. This method refers to dynamic processes associated with solvent reorganization (solvent relaxation) in response to a sudden change in charge distribution within the fluorophore upon an electronic excitation. Such excitation creates energetically unfavorable and unstable state in polar media, given by fast dipole moment transition, and is followed by reorientation of the solvent (water) molecules dissipating part of the absorbed energy to the environment (the lipid bilayer or the solvent). The energy loss is reflected in the total spectral shift of the emitted light toward longer wavelengths. This shift is

* Corresponding author. Institut UTINAM, Université de Franche-Comté, 16 Route de Gray, 25000 Besançon, France. Tel.: +33 381666482.
E-mail address: christophe.ramseyer@univ-fcomte.fr (C. Ramseyer).

0005-2736/$ – see front matter © 2010 Elsevier B.V. All rights reserved.
doi:10.1016/j.bbamem.2010.05.020

directly proportional to the polarity of the solvent. Since in lipid membranes, polarity is predominantly determined by the presence of water, the spectral shift mirrors the hydration of the membrane. Using time-resolved fluorescence instrumentation one can also follow the kinetics of the solvent rearrangement and, by this, concludes about its viscosity or local mobility in the case of lipid bilayer. Solvent relaxation in phospholipid membranes is about 10^4 times slower than in pure water, and consequently, it is very sensitive to the localization of the dye within the water–lipid interface [7,8,21,22,27]. A precise knowledge of the probe location and its stability is thus of great importance if one wants to correctly interpret solvent relaxation data. Having a set of fluorescent probes with known gradually spaced depths of locations in the bilayer allows to evaluate the amount of water and its dynamics across the membrane [7,8].

The two naphthalene derivatives presented in Fig. 1, namely Prodan (6-propionyl-2-dimethylaminonaphthalene) and Laurdan (2-dimethylamino-6-lauroylnaphthalene) are known as very useful fluorescent probes [24,28,29] due to their high sensitivity to the local polarity.

They have both an electron-donating amino group and an electron-accepting carbonyl. Prodan has a very short hydrophobic propionyl group (3 carbons). Therefore, the molecule is very mobile within the lipid membrane and can explore different locations. In fact, it was shown that, when in bilayer, Prodan locates in two distinct regions; one polar, at the interface and one less polar, at the glycerol level [30–32]. By contrast, Laurdan, with long hydrocarbon chain (12 carbons) and quaternary ammonium group attached both to its chromophore, is usually believed to be positioned at the glycerol level at a well defined location [31,33].

The experimental fluorescent SR technique gives some insights into the local membrane dynamic but again a data analysis strongly depends on the probe location. There are experimental techniques, which allow evaluation of the relative fluorophore position or its change upon membrane modification. The so-called parallax quenching method [34] relies on the determination of the distance between fluorophore and the residues that are able to alter its fluorescence. However, such approach requires also the precise knowledge of the quencher location, which in most cases, is not satisfied [35]. This intrinsic experimental difficulty may be resolved using computational methods. So far, no comprehensive works, addressing the issue of the fluorescent probe location and its alteration upon excitation have been conducted. Molecular dynamics (MD) simulations or quantum mechanical (QM) calculations can be useful tools to elucidate such question since they allow to study both the intermolecular interactions and the intra-molecular processes. Moreover, a combination of both techniques permits to observe, among other things, solvent relaxation upon electronic excitation [36]. A tremendous MD studies of lipid bilayers can be found in the literature but they do not include the fluorescent probes. In addition, only limited QM calculations were done until now for Prodan [37–45] and Laurdan [43,44]. In this work, we attempt to perform computational analysis of the two probes embedded into the lipid bilayer and to correlate our results with those recently generated with fluorescent solvent relaxation technique.

First, quantum mechanical calculations were performed to obtain correct theoretical description of Prodan and Laurdan molecules in both ground and excited states. Parameters like bond lengths, interatomic angles, partial charges [37] and general dipole moments [28,37–45] were calculated for the ground and excited states, what subsequently allows us to construct a force field for the subsequent MD simulations. Second, we have conducted MD simulations. In contrast to previous investigations on fluorescent probe molecules carried out at absolute zero temperature (0 K) and water defined as a continuum, we studied the dyes behavior at 300 K, immersed in the lipid environment. For the sake of clarity, the specific information like: absorption or emission spectra [46], the nature of the excited states, the origins of the emission process [38], detailed electronic orbital, different intramolecular charge transfer states depending on twisted or not (TICT or ICT) geometries [40,47] or multiple conformations of molecules during excitation [40] distinguished by rotational barriers [39], were not derived in the course of the present simulations.

The main objective of the present study was to characterize the interaction of fluorescence probe with the fully hydrated lipid bilayer. Our simulations were carried out for both ground and excited states. The differences in location and hydration for both dyes were compared with experimental SR data.

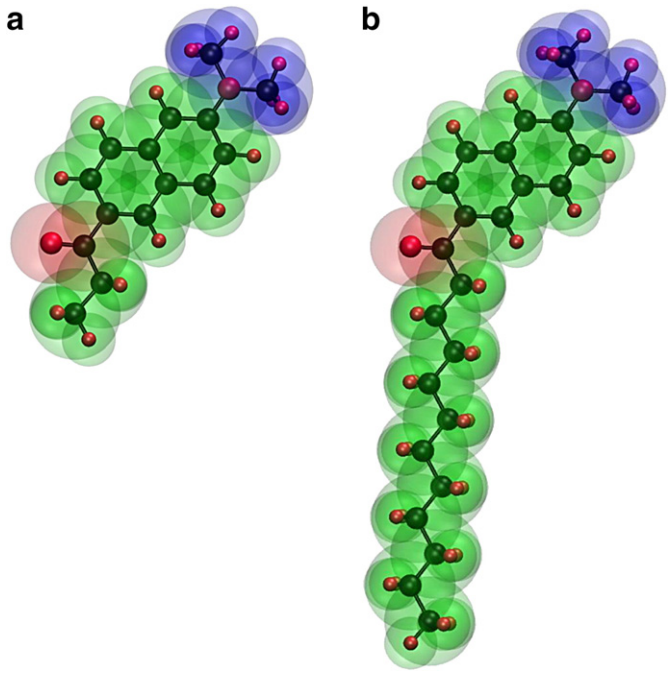

Fig. 1. Molecular structures of Prodan (a) and Laurdan (b). Transparent blue parts are the dimethylamino electron-donating groups and the transparent red subunits correspond to the carbonyl electron acceptors.

2. Methods

2.1. Quantum mechanics calculation

All quantum level calculations were performed using the Gaussian 03 software package [48]. The ground state equilibrium geometries of Prodan and Laurdan were optimized by density functional theory DFT [49,50] model with the 6-311+G(d,p) basis set. Only the planar conformation of Prodan molecule was investigated since it corresponds to the ground state geometry previously determined by X-ray analysis [51]. Since experimental data on Laurdan structure are very sparse, we decided to keep the same initial chromophore configuration as for Prodan for further optimizations. The excited states properties of fluorescent dyes were obtained from time dependent density functional theory TDDFT [52–54] with the same basis set as for DFT. The solvent effect was taken into consideration using the integral equation formalism of the polarizable continuum model IEFPCM [55–58]. In addition to structural data (bonds, angles...), we have also extracted, from the electronic structure of the molecules, other important values like dipole moments (both in ground and excited states) determined from the Mulliken charges distribution, excitation energy and oscillatory strength. We have tested different levels of theory (PM3, Hartree-Fock, DFT/TDDFT, CIS) and also derived different charge distributions (Coulson, Mulliken, NBO, Merz-Kollman, RESP). Surprisingly, we found that the Mulliken charges derived from DFT and TDDFT were the best compromise that led to the best dipole moment values when compared to the literature. Our method

of calculation gave indeed similar planar structures with only slight deformations but importantly different charges distributions and hence the right order of dipole moment modification between ground and excited states. Note that the structural differences of the dye in its ground state and excited state can also originate from the capability of a molecule to relax its structure after Franck–Condon excitation to reach the S_1 minimum potential. Note also that a multipole analysis should be more realistic to reproduce the electric potential calculated at the quantum level, especially because our results focus mainly on the replication of total dipole moment of the dye molecules. However, the introduction of such multipole expansion in MD simulations is not largely implemented in the most exploited MD codes. Supplementary analysis based on construction of the Hessian matrix (the matrix of second derivatives of the energy with respect to geometry) was also performed for further use in the force field parameterization.

2.2. Molecular dynamics simulations

The commonly used force fields that are specific databases of intra- and inter-molecular interactions include only parameters for frequently studied molecules, i.e. proteins, nucleic acids, and lipids [59–62]. Excitable molecules such as fluorescent probes are not very popular topics for computational analysis despite their relative importance for biological sciences. In this study, we have derived a correct force field for the desired molecules by following a simple protocol based on our previously validated QM analyses. Here, models of fluorescent dye molecules, Prodan and Laurdan, already optimized by quantum mechanics calculations at 0 K, were prepared using parameterization tool from the molecular graphics software VMD [63] in order to use them in further MD calculations at 300 K and under 1 atm. Due to large differences between ground (S_0) and excited (S_1) states in their electronic structures but very close geometries, we decided to keep the same intermolecular Lennard–Jones potentials for both states and to discriminate them only by their specific partial Mulliken charges distributions. In that sense, our numerical models of Prodan and Laurdan were built in order to reproduce available experimental data. During MD simulations, dyes underwent important rotations of dimethylamino groups from 0 to about $\pm 60^\circ$ and minor deformations of aromatic rings. Nevertheless, averaged trajectories give for both dyes a planar geometry consistent with QM calculations, as it was also recently observed by Morozova et al. [43].

To study the behavior of the probes in the vicinity and within lipid membrane, a DOPC lipid bilayer, composed of 72 lipids (36 per monolayer) and hydrated on each side by 35 Å water slabs, was used as an experimental model. The lipid bilayer was first generated using a pre-equilibrated lipid membrane followed by a very short energetic optimization at 0 K and then we started a long equilibration run during more than 10 ns directly at 300 K and 1 atm to be sure to reach stability and to prevent us from classical MD artifacts before inserting a fluorescent probe into the bilayer. The size of the complete systems was about $(50\times50\times100)$ Å^3. Two main simulations were conducted separately for Prodan and Laurdan molecules both initially located in the bulk water. Each of the numerical study started with the fluorophores in their ground (GS) states. After 170 ns for Prodan or 100 ns for Laurdan, when the dyes were already spontaneously incorporated into the membrane core, the first excited (EX) state was induced by change of charges distribution on the probes. From that moment, the systems with fluorophores continuously kept in their excited states were observed for further 100 ns. This protocol was employed in order to find differences between two stationary defined states. Checking the stability of the fluorescent probes locations within phospholipid bilayer and the related dynamic water behavior, many short (up to 6 ns long) supplementary simulations for the probes in EX state initially located at different depths in the membrane were also performed. These initial configurations were directly taken from the main calculations. Short (5 ps) simulation, for free fluorescent probes surrounded only by water molecules in 50^3 Å^3 box, was also conducted.

MD simulations were performed using program NAMD2.6 [62] with the CHARMM27 [64] force field containing our own extensions for fluorescent probes. All water molecules were described by the TIP3P model [65]. A constant temperature of 300 K and a constant pressure of 1 atm were ensured by Langevin dynamics and Langevin piston Nosé-Hoover algorithm [66], respectively. Chemical bonds between hydrogen and heavy atoms were constrained to their equilibrium values, long-range electrostatic forces were evaluated using the particle mesh Ewald (PME) method [67] and the integration time step was equal to 2.0 fs.

3. Results and discussion

3.1. Quantum mechanics calculation

QM simulations are generally used for extraction of specific geometric and electronic data like bond lengths, angles, dihedrals and charges distributions. Those parameters are essential for the construction of the force field used in MD simulations. The optimized ground state S_0 geometries were found to be in good agreement with available X-ray data [51]. TDDFT calculations show that the electronic structures of the excited states are completely different from S_0 despite their close geometries. A brief description of ground (S_0) and first three excited (S_1–S_3) states is given in Table 1. Calculated values of dipole moments for each state are in good agreement with those calculated by others in many experimental and computational studies [28,37–45,68]. As it was already shown, the partial electron shift from the donor to the acceptor group increases significantly the dipole moment value upon electronic excitation. For Prodan, literature shows that the ground state dipole moment can range from 4.7 to 7 D, while in the excited state, it can vary from 8.3 to even 17.4 D. In Laurdan, S_0 was found to be characterized by a dipole moment value ranging from 4.7 to 6.3 D and in the excited state—between 8.3 and 19.8 D. Moreover, information provided by TDDFT analysis on excitation energies and oscillatory strengths was crucial to decide which excited state prevails in the experimental conditions. The excitation energies are within the experimental absorption wavelength ranging from 300 to 400 nm that corresponds to excitation energies of 3.08 to 4.12 eV. Only S_1 states are used for experimental [30,69] and computational [38–41] studies since their oscillatory strengths are large compared to S_2 and S_3 for both dye molecules. Consequently, we consider only S_0 and S_1 configurations in the following MD calculations. Throughout the rest of the paper, we will label the two states as GS and EX states in order to distinguish them from the multiple states obtained from QM simulations. Moreover, the description of molecule is subsequently different for QM and MD simulations, which naturally imply a different labeling.

3.2. Molecular dynamics simulation

3.2.1. Statistics of stationary states

Initially, large scale MD simulations were performed in order to study the partition of Prodan and Laurdan between water and lipid phases. It is well known that these amphiphilic molecules easily incorporate into lipid membranes [32]. Fluorescent molecules were thus initially placed in the bulk water, far from the DOPC membrane. After 10 ns of simulations, they were found to be subsequently incorporated into the membrane and remained within the lipid bilayer for the rest of the simulation time, as shown in Fig. 2. Detailed illustration of the insertion process into lipid bilayer can be seen in animations provided in Supplementary Information. After probes incorporation, the dyes carbonyl groups are found to be positioned at the glycerol level of the lipid bilayer with their hydrocarbon chain

Table 1
Dipole moments (μ), absorption energies (E) and oscillatory strengths calculated for ground (S_0) and first three (S_1, S_2 and S_3) excited states of Prodan and Laurdan molecules.

	S_0	S_1			S_2			S_3		
	μ [D]	μ [D]	E [eV]	osc. strength	μ [D]	E [eV]	osc. strength	μ [D]	E [eV]	osc. strength
Prodan	4.96	12.91	3.10	0.5074	16.45	3.70	0.0495	17.63	3.88	0.0000
Laurdan	5.73	12.93	3.30	0.4784	16.60	3.67	0.0466	17.51	3.94	0.0001

inserted between lipid alkyl chains. The position of Laurdan (Fig. 2b) is better defined than the Prodan one (Fig. 2a), indicating a higher Prodan mobility within the membrane. Note that similar behavior was also observed for excited states (data not shown). In order to test the effect of initial dye position on this feature, additional calculations were performed for both dyes positioned in four different starting positions, i.e. at water–lipid interface, at lipid glycerol level, deep within hydrophobic lipid tails and in the center of lipid bilayer. These simulations of 30 ns each showed that the final dye position (in the GS state) do not depend on its initial position.

Single liposomal vesicle, 100 nm in diameter, contains about 10^5 of lipid molecules and up to 10^3 fluorescent probes. The experimental sample contains, thus, a large number of fluorescent molecules, whereas in the MD simulation only a limited number can be implemented. It is, indeed, difficult to analyze more than a few dyes in one sample if one wants to keep dye to lipid ratio at reasonable level (1:100). Because of that, the specific dye locations in the membrane were statistically analyzed after 10 ns following translocation from water. Both ground (GS) and excited (EX) states were kept for about 100 ns. Although unrealistic for the EX state, this allows for averaging over long trajectory substituting for statistics of many short lifetime excited states responses as in real experiment (~4 ns, depending on wavelength and environment polarity). Resulting distributions of dyes locations are presented in Fig. 3 in terms of the chromophore center distance from the bilayer center. At first glance, the histograms are broad and it is not easy to assign the most probable values. To extract them correctly, we applied Gaussian deconvolution on the histograms. Results are listed in Table 2. Prodan in its GS state can be found in three preferred locations within the membrane (see dots in Fig. 3 and for details Table 2). Two of them are equally probable while the third has only 30% of their probability. In the EX state, the dye is shifted toward the membrane surface with only one dominant location (from 14 Å in GS to 16 Å in EX). The deeper location (12 Å in GS) does not disappear completely but its occurrence decreases by a factor of two and shifts only slightly toward 13 Å. The fact that Prodan exhibits two broader distributions in the GS state, whereas in the EX state only one occurs, clearly demonstrates that the increase of the dipole moment upon excitation results with well-defined single Prodan location. Our findings are complementary with information found in literature since it was argued by experimentalists that, due to its high mobility, Prodan has two distinct locations (and orientations) within the lipid bilayer [30,32,33]. According to our best knowledge, the exact position of Prodan has not been experimentally measured. Laurdan behaves quite differently, but its location in the GS is also trimodal, as shown in Fig. 3b. Two locations are spaced by about 1 Å and have similar amplitudes, while the third (the most outer location) has the weakest contribution (see Table 2). The mean value of the two dominant locations of the dye in the GS state is equal to 11.36 Å. It matches exactly to the value determined experimentally (11.4 Å) by the parallax fluorescence quenching method [31]. Like Prodan, Laurdan in EX state shifts toward the more polar region of the bilayer and converges in a more precise location. The narrower distributions of Laurdan, in comparison to Prodan, are likely a consequence of the stabilization of its position by its longer hydrocarbon chain and quaternary ammonium group that anchor much the molecule in phospholipid bilayer.

Fluorescence solvent relaxation technique allows measuring the dynamics of dye microenvironment polarity. In case of membranes, where water molecules are bound to lipid molecules, their rearrangement in response to the dye excitation is much slower than in pure solvents. In numerical system, it is hard to quantitatively define solvent changes induced by the dye molecule since the dynamics of the dye and solvent molecules are different. They are characterized by very distinct timescales like, for instance, picoseconds for water

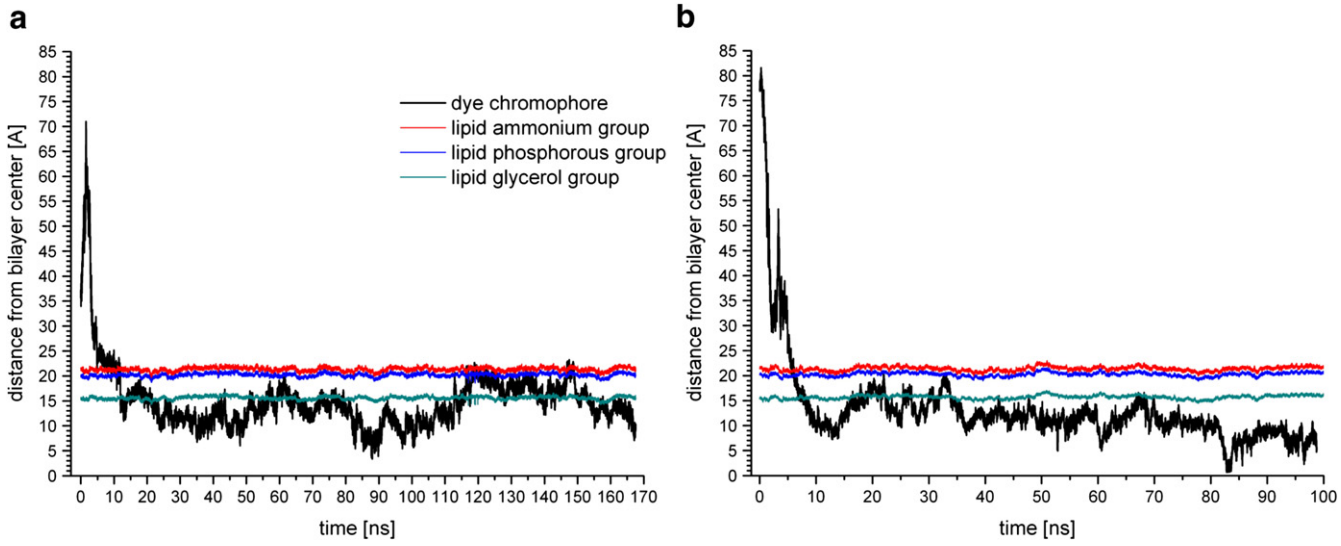

Fig. 2. The dependence of the chromophore positions at the ground state as a function of time of unconstrained MD simulation. Plot (a) shows data obtained for Prodan and plot (b) for Laurdan. Locations of the chromophore centre are depicted by black curves. The positions of ammonium (red curves), phosphorous (blue curves) and glycerol (green curves) of lipids are also plotted. Please note that simulation started with fluorescent molecule placed in the bulk water and that first 10 ns corresponds to the passive diffusion phenomenon towards the membrane surface (more details in text).

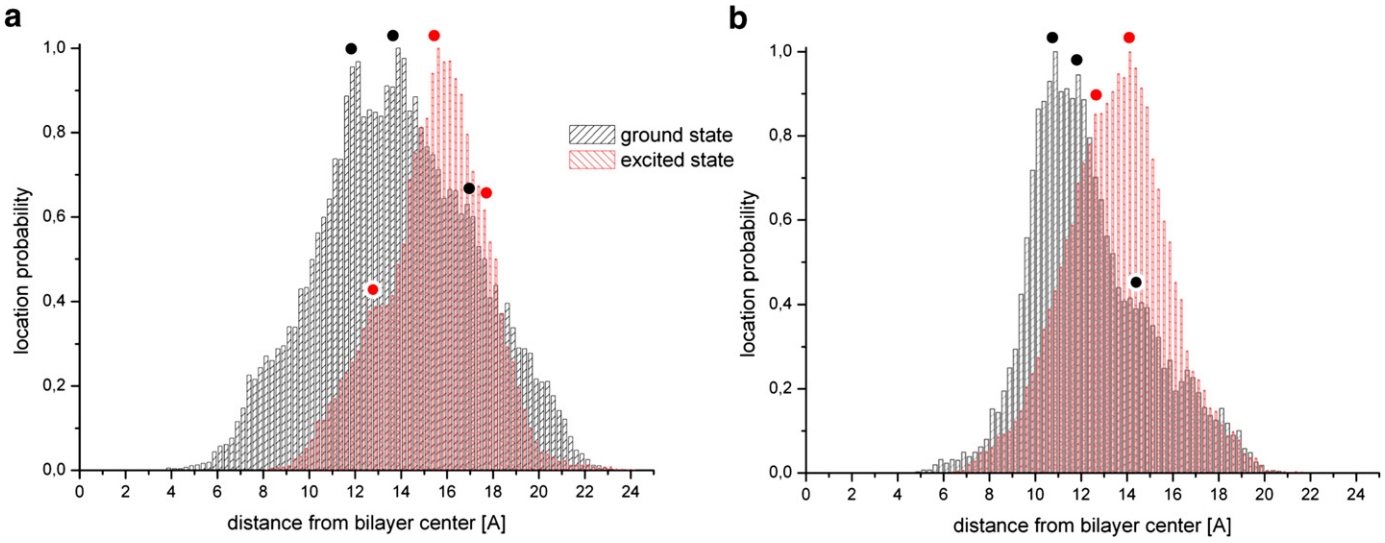

Fig. 3. Location histograms of chromophore centers of Prodan (a) and Laurdan (b) molecules in their ground (black plots) and excited (red plots) states during performed MD simulations. Positions are show as a distance from the bilayer center. Each histogram was normalized by the number of samples indicating the most probable location in given set of data. Dots correspond to the locations from Table 2.

molecule rotations and nanoseconds for dye translations. In this work, the projection of the total dipole moment vector of water molecules ($\boldsymbol{\mu}_{\mathbf{water}}$) onto the instantaneous dipole vector of dye ($\boldsymbol{\mu}_{\mathbf{dye}}$) was followed carefully. This type of treatment allows us to eliminate the effect of the dye motion in the lipid bilayer. The scalar product of these two vectors was calculated in order to quantify the water organization around the fluorescent molecule. It can have either a positive or a negative value corresponding to a parallel or an anti-parallel arrangement of both dipoles, respectively. Since the large values of the scalar product indicates a well organized water molecules, regardless of the dipoles relative orientation, the absolute value of the scalar product was used for interpretation purposes. The absolute values of the scalar averaged over 2 ns trajectories with the dyes oscillating around the most probable location within the membrane are presented in Fig. 4 as a function of the distance from the chromophore center. As expected, the effect of the dye excitation on the water arrangement is limited to its closest vicinity. For instance, Prodan in GS state directly affects its first three hydration shells occurring at 3.0, 5.5 and 9.5 Å, respectively; whereas Laurdan in GS state is able to organize only two first solvent shells at 2.5 and 4 Å from its chromophore center. For both dyes, the increase of the dipole moment upon excitation results in more organized water molecules. Additionally, the second hydration shell of Prodan in EX state is so broad that it starts to superimpose with the two adjacent water layers occurring in presence of GS state. Meanwhile, the two hydration shells of Laurdan observed in GS state merge into a single at 4 Å after dye excitation. Moreover, in contrast to Prodan, a weaker gain in water arrangement after excitation is observed. The solvent seems to be additionally altered by the substantial fluctuations of the dye, which results in less ordered configuration. This behavior may be a consequence of the long hydrocarbon tail fluctuations, which can importantly change the instantaneous dipole moment orientation of the dye at timescales even faster than the water molecules could readapt.

Table 2
Dyes locations in DOPC bilayer obtained by Gaussian deconvolution of data shown in Fig. 3. Distances (in Ångstroms) from the bilayer centre are reported with calculated normalized amplitudes of peaks (indicated by <>). GS and EX columns corresponds to ground and excited states, respectively.

Prodan location [Å]		Laurdan location [Å]	
GS	EX	GS	EX
11.97 <0.98>	12.85 <0.39>	10.84 <0.95>	
13.85 <1.00>	15.66 <1.00>	11.87 <1.00>	12.75 <0.85>
17.13 <0.28>	17.88 <0.28>	14.36 <0.41>	14.15 <1.00>

3.2.2. The dye dynamics in the excited state

The evidence of changes in dyes location upon excitation led us to analyze the dynamics of the dye translocation and the associated alterations of surrounding water molecules organization. Fluorescent probes shift toward aqueous phase is indeed a process occurring within few nanoseconds after excitation. Assuming well-converged results, independent on dye depth upon excitation, we decided to scan ten different initial positions of Prodan and Laurdan in the bilayer, selected from results of our previous simulations. The range of positions was chosen arbitrarily from 4 to 19 Å for Prodan and from 5 to 17 Å for Laurdan, which reflect ranges of locations found previously (see Fig. 3). Results presented in Fig. 5 show maps of dyes location as a function of time and for all initial configurations. Resulting dye translocations were extracted separately from each simulation as the histograms of the location probability counted on successive intervals of 0.25 ns along each collected trajectory. Then, histograms coming from each of 10 simulations of a given dye, and corresponding to the same time intervals, were summed up and normalized by the number of samples indicating the most probable location. Finally, such prepared data were gathered interval by interval in order to obtain a statistically relevant three-dimensional plot. The starting time was selected to be the instant of excitation when the dye dipole is changed. Prodan molecule shows a bimodal distribution with two main locations of 11.5 Å and 16 Å during the first 3 ns after excitation. All the molecules with the initial location higher than 14 Å occupy the position at 16 Å. The lower mode, taken by initially deeply inserted molecules, merges with the upper mode after 3.5 ns after excitation and then both converge toward the new location at around 15 Å. This may be already recognized as the preferred location found for Prodan in the EX state (Fig. 3). The Laurdan molecule, after first 3 ns of excitation, tends to reach directly the most probable position found for the EX state (around 15 Å). However, another stable location at around 12 Å remains after 3.5 ns. It could mean that Laurdan needs more than 6 ns to fully reach its statistically defined location showed in Fig. 3. Large majority of sampled dyes appear to change their position during 3–4 ns after the electronic excitation. Fluorescent molecules embedded deeply in the membrane relocate toward the

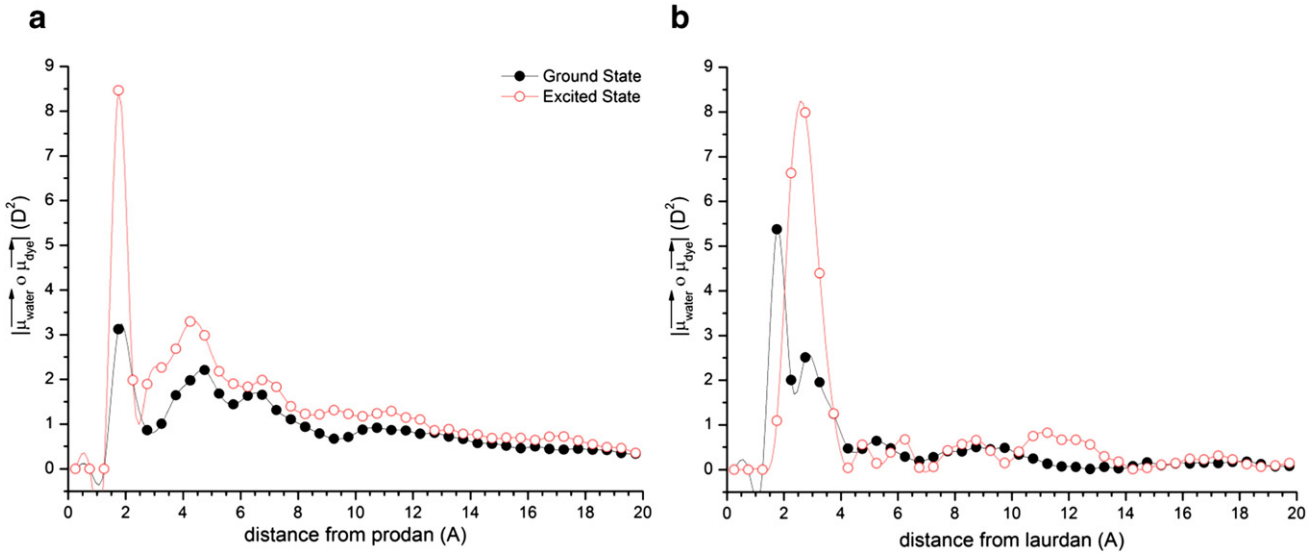

Fig. 4. Water arrangement around dye molecules, embedded into DOPC bilayer model, averaged over two consecutive nanoseconds of simulations. The absolute values of projected total water dipole vector onto Prodan (a) or Laurdan (b) dipole vector (abscissa scales), are plotted as a function of distance from the chromophore center. The bigger value means higher water organization in respect to the instantaneous probe dipole configuration.

bilayer surface driven by searching the more energetically favorable polar surrounding. The time of this movement is closely connected with the initial dye position. Nevertheless, the performed analysis is only a scan of all the range of locations with unique molecule but do not take into account an initial probability distribution as shown in Fig. 3.

3.2.3. The water dynamics after dye excitation

Because the dye response is directly linked to the presence of the polar solvent, we decided also to follow the water behavior in a similar way as during a solvent relaxation experiment. Figs. 6 and 7 present the projection of the total water dipole vector on the instantaneous dye dipole vector as a function of time, after the excitation. Trying to validate our analysis procedure, we have first simulated Prodan and Laurdan molecules inserted in the water box mimicking the bulk water. Next, the hydrated bilayer was introduced with dye molecules initially located at the same depths as indicated by arrows in Fig. 5. Experimentally, the most significant parameter obtained from SR technique is the integral relaxation time value (τ) describing the solvent mobility in the sampled environment. The mean time constant measured in pure water is around 0.3 ps [70], whereas at the lipid/water interface it is 4 orders of magnitude slower reaching 2 ns [21]. Interpretation of this experimentally observed large difference, likely induced by substantial change of polarity gradient across the bilayer normal, require precise knowledge of the fluorescent markers location. Since dye molecules start to relocate toward the bulk water after excitation, the experimental results are an average over different depths in membrane. In other words, fluorescent probes during their excited state lifetimes scan a part of the lipid bilayer. Data presented in this section are, in each case, valid for only one specific position, chosen here as the most probable or the most repetitive one.

Defining a solvent relaxation phenomenon is also not straight forward since it implies many types of processes associated to the

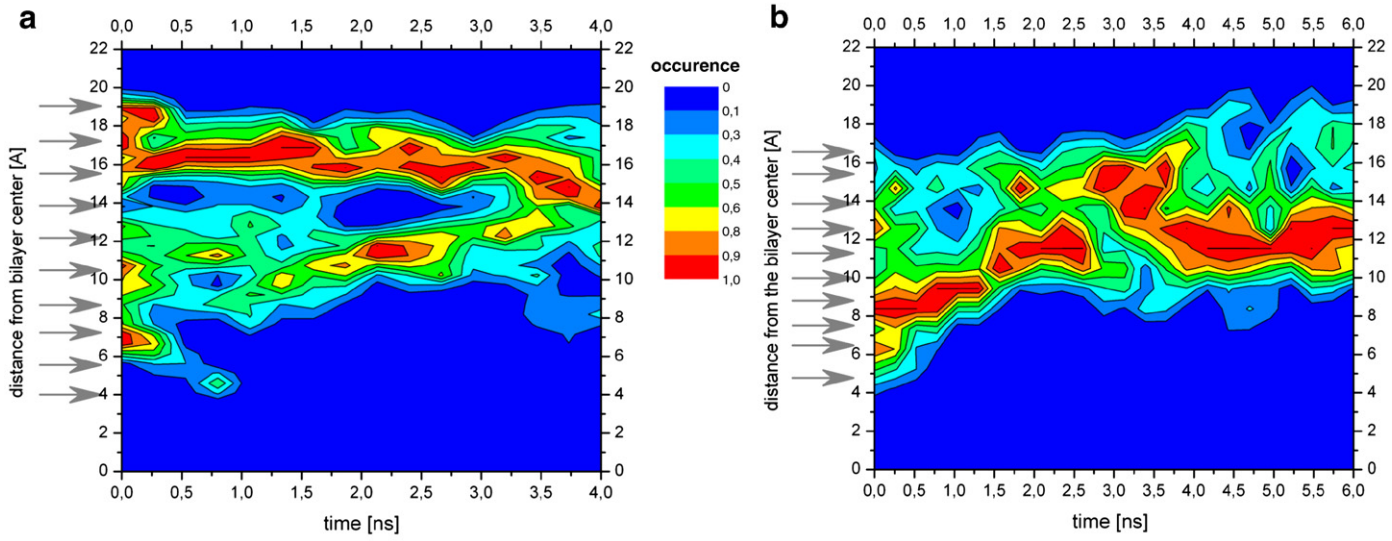

Fig. 5. Location changes of Prodan (a) and Laurdan (b) molecules after electronic excitation (starting time) merged from 10 separate MD simulations of each probe. Results are plotted as a function of time (abscissa scale) and distance from the bilayer center (ordinate scale). The unoccupied locations are colored blue whereas the most occupied are represented by red color. Arrows on the left indicate initial positions of dyes at the moment of excitation for each separately performed simulation. Please note different timescales for the two molecules.

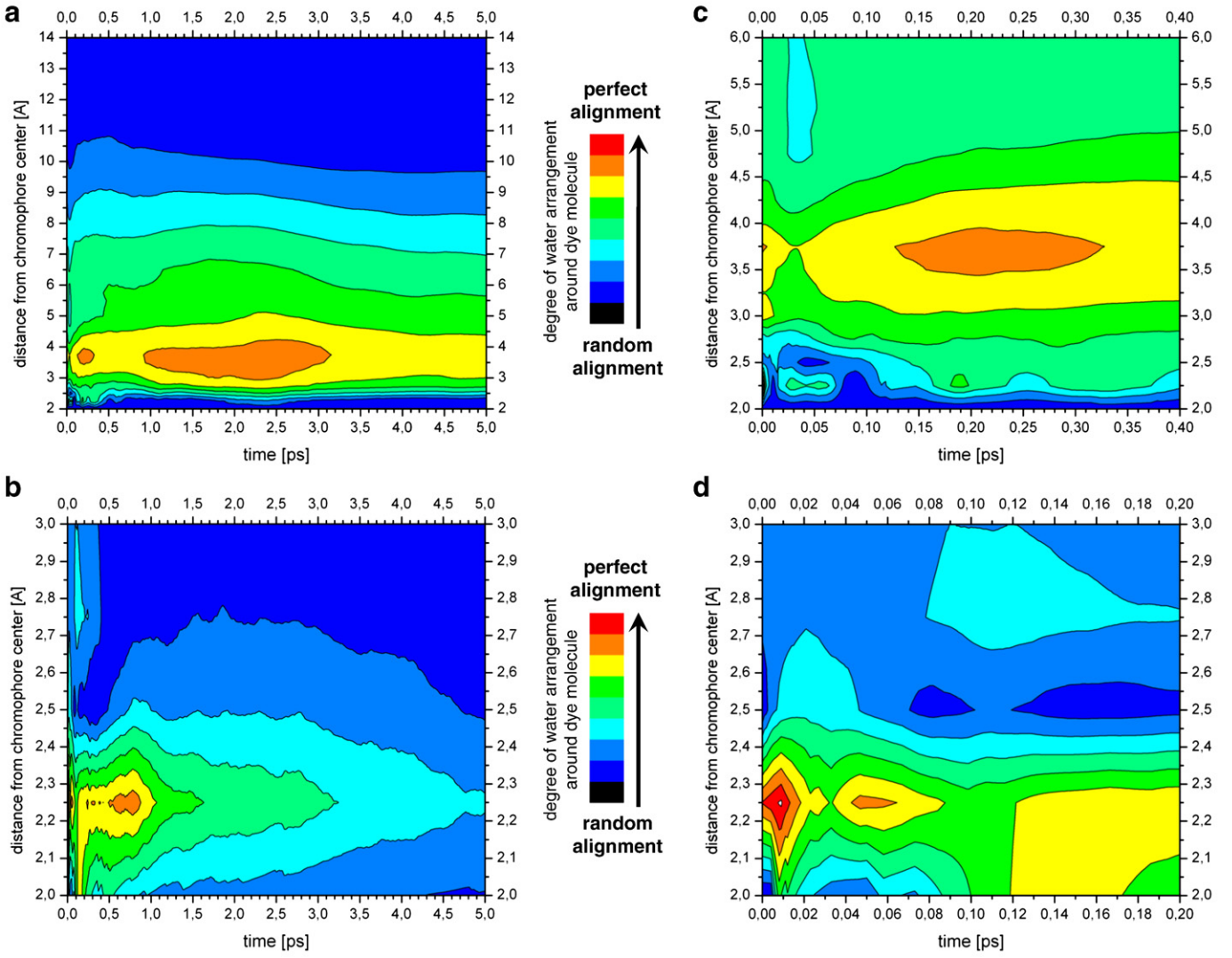

Fig. 6. Changes in dynamics of the pure water behavior around Prodan (a and c) and Laurdan (b and d) molecules, induced by fluorophore excitation. Maps were plotted as a function of time (abscissa scale) and distance from the chromophore center (ordinate scale). Blue areas indicate the lack of the water organization, green and yellow regions a progressive arrangement, while the red zones correspond to the most organized water molecules vs. dye dipole vector. Please note different scales between insets.

energy dissipation. During full atomistic simulations, we can access different levels of intramolecular energies, which are clearly distinguished by movements at separate timescales (bonds lengths oscillations, rotation or translation of the whole molecules, etc.) but in contrast to the real experiment, numerical method chosen herein give no information about interatomic energies, obviously contributing to the energy dissipation once the probe comes in the excited state. Fig. 6 presents rearrangement of bulk water around Prodan (Fig. 6a and c) and Laurdan (Fig. 6b and d) molecules after excitation. We observe that water molecules loss their induced arrangement in the picoseconds time scale, which is in excellent agreement with experimental [70] and computational [71,72] data concerning solvent relaxation in pure water. Defining one complete oscillation of water molecules (one cycle of water ordering with respect to the dye dipole, followed by an immediate disarrangement, which corresponds in Fig. 6 to the local minima of calculated vector's projections) as an important step in solvent relaxation phenomenon, we were able to link these oscillations with typical relaxation time constants (τ_i) occurring after dye excitation. All extracted times, τ_i, are listed in Table 3. In the case of Prodan, we observe three distinct cycles of water reorganization in the first hydration shell at the distance of around 3.5 Å from the chromophore center. The effect on the solvent molecules reaches up to 10 Å and is clearly visible during 5 ps of the simulation. Laurdan, in contrast, can influence only the first hydration shell at the distance of 2.0 and 2.5 Å from the chromophore center. Still three complete water-rearrangement cycles are present, but water reorganizes faster and extracted τ_i values are shorter than for Prodan. This difference is not surprising, considering that Laurdan and Prodan have the same chromophore but not the same tail, which contribute both to the dipole moment value of the dye. This first insight is in excellent agreement with earlier calculations [71,72] and experimental findings [70] justifying the applied simulation protocol. Since extracting the τ_i values depends on the definition of the limits of the whole rearrangement cycles, it was assumed that solvent relaxation process is initiated within the first water shell and then propagates on the next shells. Note that, the next relaxation cycle at a given distance (and thus for a given shell) begin before the previous one is completely propagated in the space. This can results with an overlap of cycles.

Analysis performed on numerical samples containing Prodan and Laurdan molecules, embedded into the membrane, show a strong correlation with their initial locations and initial number of water molecules in their vicinity. As mentioned before, water molecules arrangement and behavior has a preponderant role to interpret the solvent relaxation results. To quantify SR process, two parameters are determined from the time-resolved emission spectra (TRES). First,

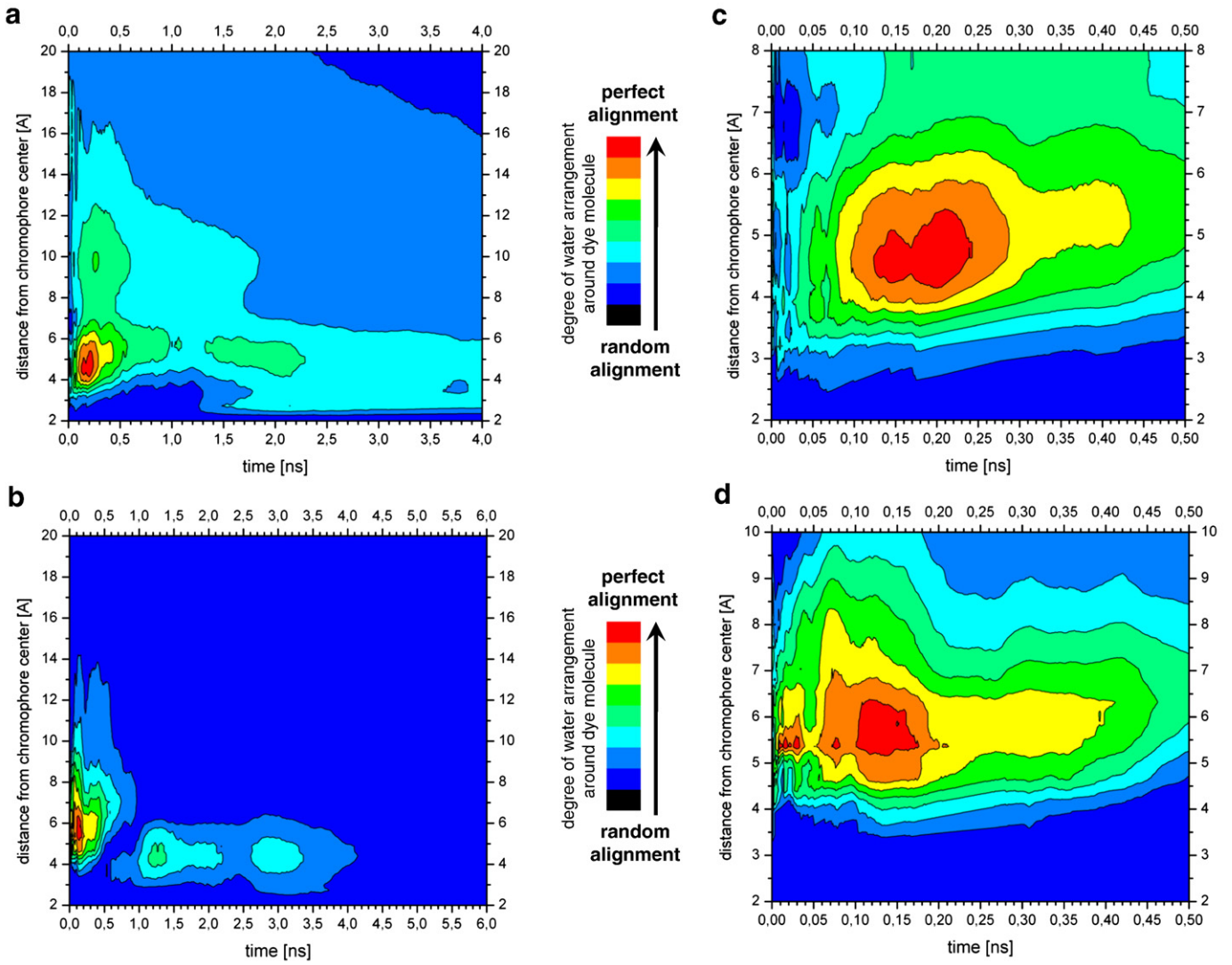

Fig. 7. Changes of water dynamics around Prodan (a and c) and Laurdan (b and d) molecules embedded into lipid membrane. Presented results correspond to the specific initial configurations of Prodan and Laurdan located at the depth of 12.2 Å and 11.4 Å, respectively. Maps were plotted as a function of time (abscissa scale) and distance from the chromophore center (ordinate scale). For color codes see Fig. 6. Please note different scales between insets.

introduced above, integrated relaxation time τ or relaxation time constants τ_i, obtained from multi-exponential fitting of the spectral response function C(t), describes mobility of water molecules. The second parameter, the total spectral shift $\Delta\nu$, is proportional to the polarity of the dye microenvironment and is believed to be correlated to the extent of membrane hydration. The most representative results, obtained for excited Prodan and Laurdan molecules when located at the distance of 12.2 Å and 11.4 Å, respectively, measured from the center of lipid bilayer are presented in Fig. 7. For Prodan only two complete cycles of water rearrangement can be clearly determined, i.e. 1.0 and 2.3 ns (Fig. 7a). However, within the first 0.5 ns after excitation (Fig. 7c) two peaks around 0.2 ns are detected. If we allow the possibility of the water rearrangement cycles to overlap, the additional local minimum could be identify at 0.17 ns after excitation, being the supplementary (third and the shortest) relaxation time in this example. The total water rearrangement take place mainly at the distance between 3 Å and 7 Å from the chromophore center but in the case of the first relaxation cycle, the effect reaches distance as far as 12 Å. Water around Laurdan presented in Fig. 7b shows three distinct cycles clearly propagating from the molecule toward the bulk water. Calculated relaxation time constants in this particular case are: 0.7, 2.2 and 3.4 ns, and again within the first half of nanosecond (Fig. 7d), there is an additional overlapping of cycles visible through a local minimum at about 0.05 ns (giving the fourth relaxation time constant in this example). The effect of excitation affects hydration shell located between 4 Å and 11 Å but after 1 ns the influence is limited only up to 6 Å.

Table 3
Relaxation time constants (τ_i) with dyes in pure water box. Values correspond to local minima from Fig. 6.

	τ_1 [ps]	τ_2 [ps]	τ_3 [ps]
Prodan	0.03	0.34	3.20
Laurdan	0.03	0.10	1.00

In addition, nine short simulations for each dye molecule in their EX states were performed to obtain statistically relevant view of solvent relaxation process after probes excitation. In those simulations, the dyes were positioned at different depths in the membrane during excitation, as illustrated by arrows in Fig. 5. In contrast to the pure water, resulting relaxation times were on the nanosecond timescale. The relaxation time constants, observed over all 20 different Prodan and Laurdan excitations, are reported in Table 4 as the intervals indicating the ranges of appeared τ_i values. We were able

Table 4
Ranges of relaxation time constants (τ_i) with dyes embedded into DOPC membrane model and gathered across multiple simulations. Please note nanosecond timescale in contrast to data shown in Table 3.

	τ_1 [ns]	τ_2 [ns]	τ_3 [ns]	τ_4 [ns]
Prodan	0.01–0.05	0.10–0.50	0.75–1.60	2.50–(more than 4.00)
Laurdan	0.01–0.05	0.16–0.60	1.25–2.50	3.00–(more than 6.00)

to find between two and four relaxation time constants τ_i for each initial configurations. The fastest rearrangement cycle occurs within the first 50 ps after excitation. Next relaxation cycle occurs during the first nanosecond. Others, much weaker, arise at later times. Relaxation times are longer for Laurdan than for Prodan, which also agrees with the experiment [21]. The results presented in this paper show that it is thus possible to retrieve kinetic parameters of solvent relaxation following excitation of fluorophore immersed in the lipid bilayer. The quantitative values calculated for two specific fluorophores, Prodan and Laurdan, match that obtained in solvent relaxation experiments, where the relaxation times constants are calculated by triple-exponential fitting fluorescent emission decays [73,74]. Moreover, a close view on the simulations reveals that the shortest time τ_1, may be attributed to the energy dissipation by rotation of water molecules. The following time τ_2 could be connected with water translation induced by dye dipole increasing upon excitation whereas the latest times (τ_3 and τ_4) are very likely determined by lipids reorganization causing subsequent impacts on water molecules. The hypothesis concerning longest times is supported by recent results of Sýkora et al. [74], showing that lipids packed in more bent vesicles, and having thus more mobile heads, exhibit faster relaxation than in large vesicles with smaller curvature.

Analysis of the changes of the amount of water around the fluorophore following excitation of dye molecules shows small difference between Prodan and Laurdan. Due to dye relocation toward surface, the number of water molecules at distance up to 5 Å from chromophore center slightly increases by 6 ± 4 for Prodan and by 9 ± 4 for Laurdan in studied cases. First hydration shell around Prodan contains thus up to 23 water molecules after dye excitation while around Laurdan there are only about 18 molecules. The overall Stokes shift $\Delta\nu$, resulting from analysis of fluorescent solvent relaxation experiment data corresponds to a polarity of a probe environment and can be directly related to the amount of water molecules involved in relaxation process. Sýkora et al. [21] have recently reported $\Delta\nu$ values equal to 3750 cm^{-1} and 3450 cm^{-1} for Prodan and Laurdan, respectively, using egg-phosphatidylcholine bilayer at ambient temperature. The higher $\Delta\nu$ value for Prodan indicates that its chromophore is in more polar surrounding, thus is surrounded by more water molecules than Laurdan, which is located deeper in the bilayer, and where less water molecules penetrate. This general tendency is also confirmed by our data.

4. Conclusions

The combination of quantum mechanical calculations (QM) and classical molecular dynamics simulations (MD) was used to characterize two fluorescent polarity sensitive probes, Prodan and Laurdan, in DOPC phospholipid membrane. A new MD protocol of dye molecules excitation was proposed for the first time. Our attempt allows extraction of important data for both ground and excited states, including impact on water and lipid molecules. Density functional theory (DFT) combined with its time dependent extension (TDDFT) enables to determine the necessary information about the chemical constitution and useful parameters for implementing MD simulations. A correct force field for the membrane fluorescent probes was thus defined for further use in MD simulations. We were able to observe passive diffusion of studied dyes from bulk water into DOPC lipid membrane. Presented statistics on dyes location along the membrane normal axis is of great importance for both experimental and theoretical studies. It reproduces the measured location of Laurdan [31] and supports the existing hypothesis of bimodal distribution of Prodan [30,32,33]. Moreover, the specific position shift toward more polar regions after excitation was observed. However, the experimental data obtained by fluorescent methods corresponds more to our results issued from the ground state than from the excited one. We suppose that marker responses during an experiment permit to uncover mostly the locations just after the excitation, still corresponding more to the ground state than for the well-established excited one. Instantaneous change of dye dipole moment, mimicking a femtosecond electronic excitation, gives also an important insight on solvent behavior. Our results show correct solvent relaxation timescales: picoseconds in pure water and nanoseconds in the headgroup region of phospholipid bilayer. We were able to observe up to four different relaxation time constants for the probes embedded into the membrane. The two shortest (τ_1 and τ_2) were associated to the rotation and translation of water molecules, respectively. The two longest time constants (τ_3 and τ_4) are very likely induced by lipids reorganization caused by previous changes in the interface hydration. The dye microenvironment mobility expressed by τ_i values could be hereby directly linked with physical phenomena occurring in measured systems. Obtained data are in excellent agreement with experimental results coming from solvent relaxation (SR) technique. In general, our computational methods allowed accessing directly typical SR parameters like relaxation time constants τ_i and shed some light on overall Stokes shift $\Delta\nu$ differences between both dyes.

Acknowledgments

Prof. Marek Langner is gratefully acknowledged for his critical reading of the manuscript. The calculations were carried out largely with the supercomputer facility at the Mésocentre a regional computational center at the University of Franche-Comté. The work was supported in part by Ministry of Education of the Czech Republic (JBK via LC06063) and Grant Agency of the Czech Republic (MH via 203/08/0114).

Appendix A. Supplementary data

Supplementary data associated with this article can be found, in the online version, at doi:10.1016/j.bbamem.2010.05.020.

References

[1] B. Baird, E.D. Sheets, D. Holowka, How does the plasma membrane participate in cellular signaling by receptors for immunoglobulin E? Biophys. Chem. 82 (1999) 109–119.
[2] D. English, Z. Welch, A.T. Kovala, K. Harvey, O.V. Volpert, D.N. Brindley, J.G.N. Garcia, Sphingosine 1-phosphate released from platelets during clotting accounts for the potent endothelial cell chemotactic activity of blood serum and provides a novel link between hemostasis and angiogenesis, FASEB J. 14 (2000) 2255–2265.
[3] F.T. Cooke, Phosphatidylinositol 3, 5-bisphosphate: metabolism and function, Arch. Biochem. Biophys. 407 (2002) 143–151.
[4] C. Luquain, V.A. Sciorra, A.J. Morris, Lysophosphatidic acid signaling: how a small lipid does big things, Trends Biochem. Sci. 28 (2003) 377–383.
[5] M. Langner, M. Przybylo, T. Borowik, A multi time-scale approach to biological systems—fluorescence studies, Pol. J. Environ. Stud. (2009).
[6] J.R. Lakowicz, Topics in Fluorescence Spectroscopy, Plenum Press, New York, 1992-2007.
[7] R. Hutterer, F.W. Schneider, H. Sprinz, M. Hof, Binding and relaxation behaviour of Prodan and Patman in phospholipid vesicles: a fluorescence and H-1 NMR study, Biophys. Chem. 61 (1996) 151–160.
[8] R. Hutterer, F.W. Schneider, W.T. Hermens, R. Wagenvoord, M. Hof, Binding of prothrombin and its fragment 1 to phospholipid membranes studied by the solvent relaxation technique, BBA-Biomembranes 1414 (1998) 155–164.
[9] A.P. Winiski, M. Eisenberg, M. Langner, S. McLaughlin, Fluorescent-probes of electrostatic potential 1-nm from the membrane-surface, Biochemistry-US 27 (1988) 386–392.

[10] M. Langner, D. Cafiso, S. Marcelja, S. McLaughlin, Electrostatics of phosphoinositide bilayer-membranes—theoretical and experimental results, Biophys. J. 57 (1990) 335–349.
[11] M. Langner, S.W. Hui, Dithionite penetration through phospholipid-bilayers as a measure of defects in lipid molecular packing, Chem. Phys. Lipids 65 (1993) 23–30.
[12] R. Hutterer, F.W. Schneider, M. Hof, Anisotropy and lifetime profiles for n-anthroyloxy fatty acids: A fluorescence method for the detection of bilayer interdigitation, Chem. Phys. Lipids 86 (1997) 51–64.
[13] B.W. Van der Meer, G. Cooker, S.Y.S. Chen, Resonance energy transfer theory and data, VCH Verlag, Weinheim, 1994.
[14] M. Langner, S.W. Hui, Merocyanine 540 as a fluorescence indicator for molecular packing stress at the onset of lamellar–hexagonal transition of phosphatidylethanolamine bilayers, BBA-Biomembranes 1415 (1999) 323–330.
[15] K. Kubica, M. Langner, J. Gabrielska, The dependence of Fluorescein-PE fluorescence intensity on lipid bilayer state. Evaluating the interaction between the probe and lipid molecules, Cell. Mol. Biol. Lett. 8 (2003) 943–954.
[16] C. Bernsdorff, A. Wolf, R. Winter, E. Gratton, Effect of hydrostatic pressure on water penetration and rotational dynamics in phospholipid-cholesterol bilayers, Biophys. J. 72 (1997) 1264–1277.
[17] G. Duportail, P. Lianos, Vesicles, Marcell Dekker, New York, 1996.
[18] R. Hutterer, A. Haefner, F.W. Schneider, M. Hof, Fluorescence microscopy and fluorescence probes, Plenum Press, New York, 1998.
[19] R. Hutterer, A.B.J. Parusel, M. Hof, Solvent relaxation of Prodan and Patman: a useful tool for the determination of polarity and rigidity changes in membranes, J. Fluoresc. 8 (1998) 389–393.
[20] R. Hutterer, M. Hof, Dynamics in diether lipid bilayers and interdigitated bilayer structures studied by time-resolved emission spectra, decay time and anisotropy profiles, J. Fluoresc. 11 (2001) 227–236.
[21] J. Sykora, P. Kapusta, V. Fidler, M. Hof, On what time scale does solvent relaxation in phospholipid bilayers happen? Langmuir 18 (2002) 571–574.
[22] P. Jurkiewicz, J. Sykora, A. Olzynska, J. Humpolickova, M. Hof, Solvent relaxation in phospholipid bilayers: principles and recent applications, J. Fluoresc. 15 (2005) 883–894.
[23] A. Sommer, F. Paltauf, A. Hermetter, Dipolar solvent relaxation on a nanosecond time scale in ether phospholipid-membranes as determined by multifrequency phase and modulation fluorometry, Biochemistry 29 (1990) 11134–11140.
[24] T. Parasassi, G. Destasio, A. Dubaldo, E. Gratton, Phase fluctuation in phospholipid-membranes revealed by Laurdan fluorescence, Biophys. J. 57 (1990) 1179–1186.
[25] S. Mukherjee, A. Chattopadhyay, Wavelength-selective fluorescence as a novel tool to study organization and dynamics in complex biological systems, J. Fluoresc. 5 (1995) 237–246.
[26] A. Chattopadhyay, Exploring membrane organization and dynamics by the wavelength-selective fluorescence approach, Chem. Phys. Lipids 122 (2003) 3–17.
[27] J. Sykora, P. Slavicek, P. Jungwirth, J. Barucha, M. Hof, Time-dependent stokes shifts of fluorescent dyes in the hydrophobic backbone region of a phospholipid bilayer: combination of fluorescence spectroscopy and ab initio calculations, J. Phys. Chem. B 111 (2007) 5869–5877.
[28] G. Weber, F.J. Farris, Synthesis and spectral properties of a hydrophobic fluorescent-probe - 6-propionyl-2-(dimethylamino)naphthalene, Biochemistry-US 18 (1979) 3075–3078.
[29] R.B. MacGregor, G. Weber, Fluorophores in polar media: spectral effects of the Langevin distribution of electrostatic interactions, Ann.N.Y.Acad.Sci. 366 (1981) 140.
[30] F. Moyano, M.A. Biasutti, J.J. Silber, N.M. Correa, New insights on the behavior of Prodan in homogeneous media and in large unilamellar vesicles, J. Phys. Chem. B 110 (2006) 11838–11846.
[31] P. Jurkiewicz, A. Olzynska, M. Langner, M. Hof, Headgroup hydration and mobility of DOTAP/DOPC bilayers: a fluorescence solvent relaxation study, Langmuir 22 (2006) 8741–8749.
[32] P.L.G. Chong, Effects of hydrostatic-pressure on the location of Prodan in lipid bilayers and cellular membranes, Biochemistry-US 27 (1988) 399–404.
[33] T. Parasassi, E.K. Krasnowska, L. Bagatolli, E. Gratton, Laurdan and Prodan as polarity-sensitive fluorescent membrane probes, J. Fluoresc. 8 (1998) 365–373.
[34] A. Chattopadhyay, E. London, Parallax method for direct measurement of membrane penetration depth utilizing fluorescence quenching by spin-labeled phospholipids, Biochemistry 26 (1987) 39–45.
[35] K.A. Kozyra, J.R. Heldt, M. Engelke, H.A. Diehl, Phase transition affects energy transfer efficiency in phospholipid vesicles, Spectrochim. Acta A 61 (2005) 1153–1161.
[36] U.F. Rohrig, I. Frank, J. Hutter, A. Laio, J. VandeVondele, U. Rothlisberger, QM/MM Car-Parrinello molecular dynamics study of the solvent effects on the ground state and on the first excited singlet state of acetone in water, Chemphyschem 4 (2003) 1177–1182.
[37] V.Y. Artukhov, O.M. Zharkova, J.P. Morozova, Features of absorption and fluorescence spectra of prodan, Spectrochim. Acta A 68 (2007) 36–42.
[38] B. Mennucci, M. Caricato, F. Ingrosso, C. Cappelli, R. Cammi, J. Tomasi, G. Scalmani, M.J. Frisch, How the environment controls absorption and fluorescence spectra of Prodan: a quantum-mechanical study in homogeneous and heterogeneous media, J. Phys. Chem. B 112 (2008) 414–423.
[39] A.B.J. Parusel, F.W. Schneider, G. Kohler, An ab initio study on excited and ground state properties of the organic fluorescence probe Prodan, J. Mol. Struc. Theochem. 398 (1997) 341–346.
[40] A. Parusel, Semiempirical studies of solvent effects on the intramolecular charge transfer of the fluorescence probe Prodan, J. Chem. Soc. Faraday T 94 (1998) 2923–2927.
[41] A.B.J. Parusel, W. Nowak, S. Grimme, G. Kohler, Comparative theoretical study on charge-transfer fluorescence probes: 6-propanoyl-2-(*N, N*-dimethylamino)naphthalene and derivatives, J. Phys. Chem. A 102 (1998) 7149–7156.
[42] A.B.J. Parusel, R. Schamschule, G. Kohler, Nonlinear optics. A semiempirical study of organic chromophores, J. Mol. Struc. Theochem. 544 (2001) 253–261.
[43] Y.P. Morozova, O.M. Zharkova, T.Y. Balakina, V.Y. Artyukhov, Effect of proton-donor solvent and structural flexibility of prodan and laurdan molecules on their spectral-luminescent properties, J. App. Spectrosc. 76 (2009) 312–318.
[44] N.A. Nemkovich, W. Baumann, Molecular Stark-effect spectroscopy of Prodan and Laurdan in different solvents and electric dipole moments in their equilibrated ground and Franck–Condon excited state, J. Photoch. Photobio. A 185 (2007) 26–31.
[45] A. Samanta, R.W. Fessenden, Excited state dipole moment of Prodan as determined from transient dielectric loss measurements, J. Phys. Chem. A 104 (2000) 8972–8975.
[46] B.C. Lobo, C.J. Abelt, Does Prodan possess a planar or twisted charge-transfer excited state? Photophysical properties of two Prodan derivatives, J. Phys. Chem. A 107 (2003) 10938–10943.
[47] M. Novaira, M.A. Biasutti, J.J. Silber, N.M. Correa, New insights on the photophysical behavior of Prodan in anionic and cationic reverse micelles: from which state or states does it emit? J. Phys. Chem. B 111 (2007) 748–759.
[48] M.J. Frisch, G.W. Trucks, H.B. Schlegel, G.E. Scuseria, M.A. Robb, J.R. Cheeseman, J. Montgomery, J. A., T. Vreven, K.N. Kudin, J.C. Burant, J.M. Millam, S.S. Iyengar, J. Tomasi, V. Barone, B. Mennucci, M. Cossi, G. Scalmani, N. Rega, G.A. Petersson, H. Nakatsuji, M. Hada, M. Ehara, K. Toyota, R. Fukuda, J. Hasegawa, M. Ishida, T. Nakajima, Y. Honda, O. Kitao, H. Nakai, M. Klene, X. Li, J.E. Knox, H.P. Hratchian, J.B. Cross, V. Bakken, C. Adamo, J. Jaramillo, R. Gomperts, R.E. Stratmann, O. Yazyev, A.J. Austin, R. Cammi, C. Pomelli, J.W. Ochterski, P.Y. Ayala, K. Morokuma, G.A. Voth, P. Salvador, J.J. Dannenberg, V.G. Zakrzewski, S. Dapprich, A.D. Daniels, M.C. Strain, O. Farkas, D.K. Malick, A.D. Rabuck, K. Raghavachari, J.B. Foresman, J.V. Ortiz, Q. Cui, A.G. Baboul, S. Clifford, J. Cioslowski, B.B. Stefanov, G. Liu, A. Liashenko, P. Piskorz, I. Komaromi, R.L. Martin, D.J. Fox, T. Keith, M.A. Al-Laham, C.Y. Peng, A. Nanayakkara, M. Challacombe, P.M.W. Gill, B. Johnson, W. Chen, M.W. Wong, C. Gonzalez, J.A. Pople, I. Gaussian, Gaussian 03, Revision C.02, in, Wallingford CT, 2004.
[49] P. Hohenberg, W. Kohn, Inhomogeneous electron gas, Phys. Rev. B 136 (1964) B864.
[50] W. Kohn, L.J. Sham, Self-consistent equations including exchange and correlation effects, Phys. Rev. 140 (1965) 1133.
[51] P. Ilich, F.G. Prendergast, Singlet adiabatic states of solvated Prodan—a semiempirical molecular-orbital study, J. Phys. Chem.-US 93 (1989) 4441–4447.
[52] R.E. Stratmann, G.E. Scuseria, M.J. Frisch, An efficient implementation of time-dependent density-functional theory for the calculation of excitation energies of large molecules, J. Chem. Phys. 109 (1998) 8218–8224.
[53] R. Bauernschmitt, R. Ahlrichs, Treatment of electronic excitations within the adiabatic approximation of time dependent density functional theory, Chem. Phys. Lett. 256 (1996) 454–464.
[54] M.E. Casida, C. Jamorski, K.C. Casida, D.R. Salahub, Molecular excitation energies to high-lying bound states from time-dependent density-functional response theory: characterization and correction of the time-dependent local density approximation ionization threshold, J. Chem. Phys. 108 (1998) 4439–4449.
[55] E. Cances, B. Mennucci, J. Tomasi, A new integral equation formalism for the polarizable continuum model: theoretical background and applications to isotropic and anisotropic dielectrics, J. Chem. Phys. 107 (1997) 3032–3041.
[56] B. Mennucci, E. Cances, J. Tomasi, Evaluation of solvent effects in isotropic and anisotropic dielectrics and in ionic solutions with a unified integral equation method: theoretical bases, computational implementation, and numerical applications, J. Phys. Chem. B 101 (1997) 10506–10517.
[57] J. Tomasi, B. Mennucci, E. Cances, The IEF version of the PCM solvation method: an overview of a new method addressed to study molecular solutes at the QM ab initio level, J. Mol. Struc. Theochem. 464 (1999) 211–226.
[58] B. Mennucci, J. Tomasi, Continuum solvation models: a new approach to the problem of solute's charge distribution and cavity boundaries, J. Chem. Phys. 106 (1997) 5151–5158.
[59] B.R. Brooks, R.E. Bruccoleri, B.D. Olafson, D.J. States, S. Swaminathan, M. Karplus, CHARMM: a program for macromolecular energy, minimizations, and dynamics calculations, J. Comp. Chem. 4 (1983) 187–217.
[60] E. Lindahl, B. Hess, D. van der Spoel, GROMACS 3.0: a package for molecular simulation and trajectory analysis, J. Mol. Model. 7 (2001) 306–317.
[61] D.A. Case, T.A. Darden, T.E. Cheatham III, C.L. Simmerling, J. Wang, R.E. Duke, R. Luo, K.M. Merz, B. Wang, D.A. Pearlman, M. Crowley, S. Brozell, V. Tsui, H. Gohlke, J. Mongan, V. Hornak, G. Cui, P. Beroza, C. Schafmeister, J.W. Caldwell, W.S. Ross, P.A. Kollman, AMBER 8, University of California, San Francisco, 2004.
[62] J.C. Phillips, R. Braun, W. Wang, J. Gumbart, E. Tajkhorshid, E. Villa, C. Chipot, R.D. Skeel, L. Kale, K. Schulten, Scalable molecular dynamics with NAMD, J. Comput. Chem. 26 (2005) 1781–1802.
[63] W. Humphrey, A. Dalke, K. Schulten, VMD—visual molecular dynamics, J. Molec. Graphics 14 (1996) 33–38.
[64] A.D. MacKerell, D. Bashford, M. Bellott, R.L. Dunbrack, J.D. Evanseck, M.J. Field, S. Fischer, J. Gao, H. Guo, S. Ha, D. Joseph-McCarthy, L. Kuchnir, K. Kuczera, F.T.K. Lau, C. Mattos, S. Michnick, T. Ngo, D.T. Nguyen, B. Prodhom, W.E. Reiher, B. Roux, M. Schlenkrich, J.C. Smith, R. Stote, J. Straub, M. Watanabe, J. Wiorkiewicz-Kuczera, D. Yin, M. Karplus, All-atom empirical potential for molecular modeling and dynamics studies of proteins, J. Phys. Chem. B 102 (1998) 3586–3616.
[65] W.L. Jorgensen, J. Chandrasekhar, J.D. Madura, R.W. Impey, M.L. Klein, Comparison of simple potential functions for simulating liquid water, J. Chem. Phys. 79 (1983) 926–935.
[66] S.E. Feller, Y.H. Zhang, R.W. Pastor, B.R. Brooks, Constant-pressure molecular-dynamics simulation—the Langevin piston method, J. Chem. Phys. 103 (1995) 4613–4621.
[67] T. Darden, D. York, L. Pedersen, Particle mesh Ewald: an N.log(N) method for Ewald sums in large systems, J. Chem. Phys. 98 (1993) 10089–10092.

[68] J. Catalan, P. Perez, L. J., B. G.F., Analysis of the solvent effect on the photophysics properties of 6-propionyl-2-(dimethylamino)naphthalene (PRODAN), J. Fluoresc. 1 (1991) 215–223.
[69] C.E. Bunker, T.L. Bowen, Y.P. Sun, A photophysical study of solvatochromic probe 6-propionyl-2-(n, n-dimethylamino)naphthalene (Prodan) in solution, Photochem. Photobiol. 58 (1993) 499–505.
[70] R. Jimenez, G.R. Fleming, P.V. Kumar, M. Maroncelli, Femtosecond solvation dynamics of water, Nature 369 (1994) 471–473.
[71] M. Maroncelli, G.R. Fleming, Computer-simulation of the dynamics of aqueous solvation, J. Chem. Phys. 89 (1988) 5044–5069.
[72] M. Maroncelli, Computer-simulations of solvation dynamics in acetonitrile, J. Chem. Phys. 94 (1991) 2084–2103.
[73] R. Sachl, M. Stepanek, K. Prochazka, J. Humpolickova, M. Hof, Fluorescence study of the solvation of fluorescent probes prodan and laurdan in poly(epsilon-caprolactone)-block-poly(ethylene oxide) vesicles in aqueous solutions with tetrahydrofurane, Langmuir 24 (2008) 288–295.
[74] J. Sykora, P. Jurkiewicz, R.M. Epand, R. Kraayenhof, M. Langner, M. Hof, Influence of the curvature on the water structure in the headgroup region of phospholipid bilayer studied by the solvent relaxation technique, Chem. Phys. Lipids 135 (2005) 213–221.